2_C19

Automated Fault Detection Strategy on Virtual In-situ Calibration Building Energy System: Partition of Calibration Domain

Peng Wang **Jiteng Li** **Sungmin Yoon**

Tianyi Zhao **Yuebin Yu**

ABSTRACT

Sensor errors have an important impact on the operation, control, and detection of building energy systems. Correct and reliable sensors can effectively reduce the energy consumption of building energy systems. Virtual in-situ calibration (VIC) based on Bayesian inference and Markov Chain Monte Carlo method that no need to increase extra or install new sensors can effectively reduce systematic error and random error of the sensor and increase the reliability. However, due to the long calibration time, large amount of data, normalization constant and sensitivity coefficient required for the Whole calibration and Local calibration previously studied by the research group, all the sensors could not be fully calibrated or the calibration results were unstable. Based on the above problems, we proposed a new calibration method -- Component calibration, which divides the complex building energy system into several components to achieve accurate calibration without various coefficients, few data and calibration time. First, these three methods are applied to the actual primary air return reheating system, and the accuracy of Component calibration method is verified by comparing the results of the three calibration methods. Then, different results generated by different division of Local calibration domain are compared, which verifies from the side that Component calibration can perfectly calibrate systematic errors and random errors of all sensors.

1. Introduction

With the continuous development of the economy and society, the process of urbanization is accelerating. A large number of people have migrated to the cities, thereby causing significant stress to the cities' housing infrastructure [1]. Super high-rise buildings have become the first choice to relieve this stress and address the scarcity of land area [2]. With the deepening of the complexity of building structures, the building energy systems for heating, ventilation, air condition, and refrigeration (HVAC&R) are becoming more complex. Statistics show that HVAC&R systems are widely used in civil and commercial buildings, industrial plants, data centers, etc. For example, the energy consumption of HVAC&R systems in buildings usually account for 50–60% of their total energy consumption [3-5]. To solve the problem of high energy consumption in building systems, various control methods are usually used for intelligent adjustment, such as continuous fine tuning [6], analysis optimization [7, 8], and fault detection and diagnosis based on building automation systems [9- 13].

At present, various traditional methods are being used to calibrate sensors of building energy systems [14-16]. In the existing literature, model-based and data-driven sensor fault diagnosis methods have received much attention. However, these traditional methods have the following two practical problems in the calibration process: 1) only focusing on a single fault. The building energy system is complex in structure, and the sensors are connected with each other. In the process of operation, the fault of one sensor may lead to several sensor faults in succession owing to a chain reaction, and the diagnosis of concurrent faults of multiple sensors is unavailable at present. 2) Existing sensor fault diagnosis methods only focus on diagnosis and do not involve repair. After the building energy system has been running for a period of time, the sensors drift to different degrees. Repair on the basis of successful diagnosis is a problem that requires attention. Hence, our research group has introduced the virtual in-situ calibration (VIC) method into the sensor network to calibrate the systematic and random error generated during the sensor operation [17-19]. In particular, the VIC method can solve the following problems[20]: 1) excess cost and time, 2) the normal operation of the system being interrupted, 3) difficulties in removal and installation, and 4) the complex structure of the sensor network. There are numerous and complicated sensors in building energy systems, and traditional methods cannot solve the different systematic and random errors that sensors may produce in different environments [14]. However, the VIC method combines historical data with the model of the system according to basic theorems such as energy conservation and mass conservation. On the basis of not removing or installing new sensors, the systematic errors generated in different working environments and random errors generated owing to sensor aging can be calibrated simultaneously.

In previous studies[17], our research group has proposed the idea of whole and local calibration based on the existing building energy system. The whole calibration method is to set the complete building energy system into a calibration domain when all sensors of the system are calibrated. Subsequently, based on sensitivity analysis and historical experience

Peng Wang, Jiteng Li and Tianyi Zhao are affiliated with Dalian University of Technology, Dalian City, China. **Sungmin Yoon** is affiliated with Incheon National University Incheon, Republic of Korea. **Yuebin Yu** is affiliated with University of Nebraska-Lincoln, Omaha, United States.

[21], all sensor and system models are built into a function for calibration. Although it is relatively simple to define the calibration domain, this method often results in poor calibration results due to considerable requirement of historical data and correlation coefficients. In order to improve the accuracy of calibration, our research group later introduced local calibration into the sensor calibration of the system. The complete building energy system is divided into two parts, and then based on sensitivity analysis and historical experience, the sensor network is divided into two parts and calibrated in turn. Compared with whole calibration, this method simplifies sensitivity analysis owing to the reduction in parameters in each equation. Simultaneously, it halves the historical data required for calibration, thereby improving the calibration accuracy and applicability of calibration. However, the determination of sensitivity and normalizing coefficients in these two methods is significantly difficult. The determination of the normalizing coefficient is usually based on experience, while the sensitivity coefficient is obtained through a series of complex algorithms, such as the genetic algorithm(GA), which has been discussed in our previous study [22]. This leads to a strong randomness of these two parameters and unsatisfactory calibration results. Each local calibration domain still contains a large number of sensors in more complex building energy systems. The accuracy of calibration results will be significantly reduced when the number of historical data is small.

To address the drawbacks of the above two calibration methods, this study proposes a new sensor calibration domain division method termed as component calibration. The complete building energy system is divided into several interrelated small parts, which are then regarded as components and calibrated separately. Component calibration has considerable advantages. First, each component contains only two or three sensors; hence, the equations are simple, and the calibration result is very robust and ideal. Second, it’s not necessary to calculate the sensitivity and normalizing coefficients; hence, the operation time is relatively less. Third, the calibrated data can be substituted into another component associated with it. This is due to the correlation between the components, thereby significantly improving the calibration accuracy of the next component related to it.

2. Virtual in-situ sensor calibration

2.1 Bayesian inference

During the sensor calibration process, the Bayesian inference is used to seek the minimum value of the distance function D(x) and solve the offsetting constants and unknown parameters in the sensor network. According to Bayesian theory, the posterior distribution $P(x|Y_b)$ of variable x (offsetting constants and unknown parameters) is calculated based on the prior distribution $\pi(x)$ and likelihood function $P(Y_b|x)$, as shown in Eq. (1). For the three calibration methods mentioned above, their prior distribution $\pi(x)$ follows the Gaussian distribution and could be estimated from the Central Limit Theorem [23]. The mean value and standard deviation in the Gaussian distribution can be obtained from the physical characteristics of the sensors. The precision of each sensor can be regarded as the standard deviation of prior distribution, but since there is no strong connection between the mean value and the standard deviation, the mean value cannot be calculated. The mean value is a critical parameter for the prior distribution and it could be set to zero (no systematic error). For the unknown parameters in the equation, their mean value and standard deviation are obtained through references or expert knowledge. As shown in Eq. (2), the likelihood function $P(Y_b|x)$ is formed by inserting the distance functions D(x) of the whole, local, and component calibration into the Gaussian distribution, respectively. When the distance function D(x) is minimum, the likelihood function $P(Y_b|x)$ becomes maximum.

$$P(x|Y_b) = \frac{P(Y_b|x)\times\pi(x)}{P(Y_b)} \tag{1}$$

$$P(Y_b|x) = \frac{1}{\sigma\sqrt{2\pi}}\exp\left[-\frac{1}{2\sigma^2}D(x)\right] \tag{2}$$

$$P(Y_b) = \int P(Y_b|x)\pi(x)\,dx \tag{3}$$

where x are the variables, Y_b is the benchmark function, $D(x)$ is the distance function, $P(Y_b)$ is the normalizing constant, σ is the standard deviation, and $\pi(x)$, $P(x|Y_b)$, and $P(Y_b|x)$ are the prior distribution, posterior distribution, and likelihood function of the variables, respectively.

As shown in Eq. (3), it is usually difficult to calculate the normalizing constant $P(Y_b)$ analytically, but the posterior distribution $P(x|Y_b)$ can be derived by constructing Markov Chains, thereby effectively avoiding complicated integration. In this study, the Metropolis-Hastings algorithm in Monte Carlo (MCMC) is used to obtain a series of random samples from a joint multivariate distribution [24], and then the posterior distribution of offset constants and unknown parameters is calculated.

2.2 Distance function for VIC method

When the VIC method is used to calibrate the sensors, the key problem of calibration is to incorporate the distance function into the likelihood function, where the distance function represents the difference between the correction functions and benchmarks for working sensors in a system. The distance functions of whole, local and component calibration are shown in Eqs. (4)-(6). Since the local calibration divides the whole calibration into two or three parts, there are fewer models in the calibration domain than the whole domain ($k < j$). In addition, the overall system is divided into several small parts for component calibration, and each part contains only one model. Compared with the whole and local calibrations, there is no sensitivity or normalizing coefficient for multiple models in the component calibration domain. According to the above definition, when the measurement of the sensor is highly accurate, then a distance function close to zero is obtained. The benchmark can be calculated by reliable output variables (e.g. refrigerating capacity, heating capacity, etc.) or calibration functions of relevant working sensors, as shown in Eq. (7). Simultaneously, the measurement value of the working sensor is compensated for the systematic error generated by the sensor in the measurement process by adding an offsetting constant for the calibration function defined by Eq. (8). The variables to be solved in the sensor calibration process include the offsetting constant (x) of all corrected functions and the unknown parameter (x_u) of the benchmark function.

During the operation of the building energy system, the temperature and humidity sensors work at all times, hence there are too many offsetting constants (x) and unknown parameters (x_u) inside the system models, making the solution of the distance function a non-positive definite problem. In order to improve the accuracy of sensor calibration, it is necessary to establish multiple sets of steady-state measurement sets (T) to increase the number of equations. The whole system can also be divided into several local or component calibration domains to reduce the number of offsetting constants (x) and unknown parameters (x_u) so that the results are closer to the true values.

$$D^W(x) = \sum_{i=1}^{I}\sum_{j=1}^{J} n_h s_h (Y_{R,h} - Y_{b,h})^2 \tag{4}$$

$$D^L(x) = \sum_{i=1}^{I}\sum_{k=1}^{K} n_k s_k (Y_{R,k} - Y_{b,k})^2 (k < j) \tag{5}$$

$$D^C(x) = \sum_{i=1}^{I}(Y_R - Y_b)^2 \tag{6}$$

$$Y_b = f(Y_{c1}, Y_{c2}, \ldots, Y_{cr}, x_{u1}, x_{u2}, \ldots, x_{uq}) \tag{7}$$

$$Y_c = g(M, x_1, x_2, \ldots, x_k) \tag{8}$$

where $D^W(x)$, $D^L(x)$, $D^C(x)$ are the distance functions for the whole, local and component calibrations, respectively, x is the offsetting constant, i and I are the number of data sets, j and J are the number of system components in whole calibration, k and K are the number of system components in local calibration, n is the normalizing coefficient, s is the sensitivity coefficient, M is the measurement from sensors, Y_{cr} is the measurement after correction, x_{uq} are the unknown parameters, Y_R and Y_b are the outputs of reliable and benchmark, respectively, f is a system model, and g is a correction function.

3. Partition of different calibration domains

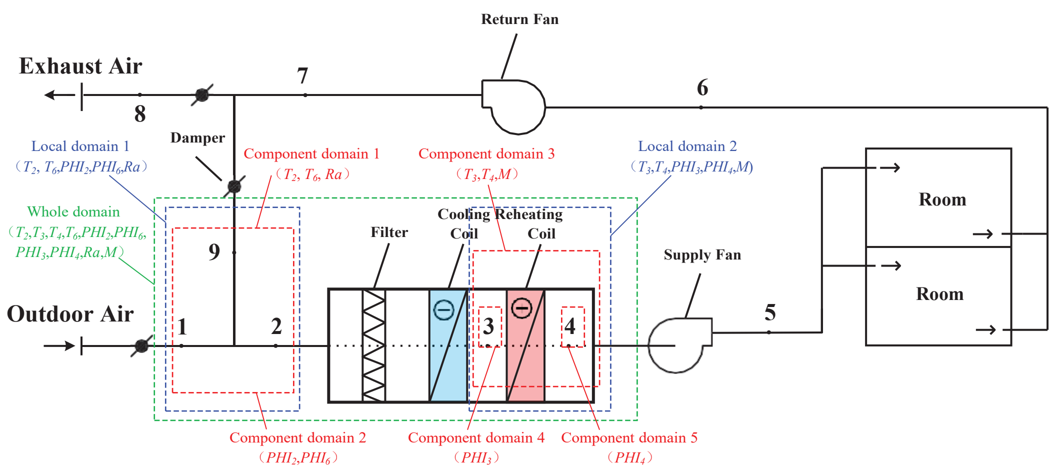

Fig.1. Air handling unit system and partition of different calibration domains

For the three different errors analyzed above, the traditional method cannot accurately identify and repair. In this article, the VIC method proposed by our research group is used to calibrate the three different errors based on the three calibration methods. First, the air handling unit system is defined as a calibration domain for whole calibration, which includes all temperature sensors, humidity sensors, fresh air ratio and mass flow rates. In addition, the offsetting constants generated by all sensors and some unknown parameters (mass flow rate, fresh air ratio and humidity of point 3) in the system are incorporated into a distance function $D^W(x)$ to minimize it, thus obtaining the offsetting constants of all sensors and the values of unknown parameters.

We divide the whole system into two parts based on sensitivity analysis and importance ranking of inputs and outputs for local calibration, and these two parts are calibrated in turn. The first calibration domain refers to the mixing phase, which includes the return air temperature T_6, return air humidity PHI_6, mixing air temperature T_2, mixing air humidity PHI_2 and fresh air ratio Ra. Equipments can be used easily to measure the fresh air temperature T_1 and fresh air humidity PHI_1 outside, thereby it's assumed there's no error in these two parameters. In the first calibration domain, the energy conservation and mass conservation equations are used to construct the benchmark function and the correction function of h_2. They are incorporated into a distance function $D^L(x)$ that is to be solved, so that the systematic and random errors of T_2, T_6, PHI_2, PHI_6 and the values of unknown parameters Ra are calculated. The second calibration domain refers to the cooling and reheating stages, and includes the air temperature T_3 and air humidity PHI_3 treated by the surface cooler, air supply temperature T_4 and the air supply humidity PHI_4 after passing through the reheater, and the mass flow rate M. Subsequently, based on T_2 and PHI_2 that have been calibrated in the first calibration domain, the benchmark function and correction function of the cooling capacity Q_c and reheat capacity Q_h are constructed and incorporated into the distance function $D^L(x)$, thus calculating the systematic and random errors of T_3, T_4 and PHI_4 and the values of unknown parameters PHI_3 and M.

Compared with the above two calibration methods, component calibration divides the system into five calibration domains, each of which contains up to three variables. The reduction of the number of variables can not only increase the accuracy, but also decrease the number of required historical data, thus significantly increasing the applicability of the VIC method. The first calibration domain includes three parameters, namely mixed air temperature T_2, return air temperature T_6, and fresh air ratio Ra. The benchmark function Y_b and distance function $D^C(x)$ of the mixed air temperature sensor are constructed by using the proportional relation between the fresh air and return air, thus the errors of the three variables are obtained from the posterior distribution. The second calibration domain consists of mixed air humidity PHI_2 and return air humidity PHI_6, and they are calibrated based on the calibrated sensor measurements (T_2, T_6, Ra) in the first calibration domain. For the third calibration domain, the temperatures T_3, T_4 before and after the reheater and the mass flow M in the pipeline need to be calibrated. Here, we use the energy Q_h on the hot water side of the reheater as a benchmark. Subsequently, we construct the correction functions of the temperatures T_3, T_4 and unknown parameters M according to the energy conservation equation, thus obtaining the distance function $D^C(x)$ of the calibration domain. For the air handling unit system, the humidity behind the surface cooler is generally the dew point humidity that is approximately 0.9-0.95, but the specific value is unknown. The unknown parameter PHI_3 is assumed to be in the fourth calibration domain, and the specific value of PHI_3 is obtained by the previously calibrated T_2, T_3, PHI_2, M values and the general calculation method of air physical property parameters. Similarly, for the last calibration domain, there is only one humidity sensor PHI_4. Based on the local domains 3 and 4, the benchmark equation Y_b and distance equation $D^C(x)$ of PHI_4 are established. Based on the above division of calibration domains, all sensors and unknown parameters of the entire air handling unit system are calibrated, and the specific results are shown in Fig. 1.

4. Results and discussions

4.1 Results for the three calibration methods

The accuracy of calibration results is expressed by the mean and standard deviation of the posterior distribution. Before calibration, it is generally considered that the mean value (systematic error) of the prior probability of sensor error is zero (no systematic error), and the standard deviation (random error) is the precision of the sensor, as the sensor operates smoothly in the building energy system. For the required values without sensors installed in the system, the mean and standard deviation of the prior probability are usually obtained according to historical experience or relevant documents. We gradually correct the prior distribution set at the beginning to a reasonable posterior distribution through the system model and a series of steady-state measurement values of sensors based on the Bayesian and MCMC methods, thus obtaining the systematic and random errors of all sensors in the system that are to be repaired. The real-time and on-line repair of all sensors in the system is realized by not removing the existing sensors and installing new ones, thereby saving manpower and material resources and ensuring the stable operation of the system. As shown in Table 2, different ranges of systematic errors (30%, 20%, 10%) and random errors (15%, 10%, 5%) and different calibration methods (whole calibration, local calibration, component calibration) are set for Cases 1-3. After calibration by the VIC method, the temperature, humidity, and unknown parameters (PHI_3, Ra, M) are corrected to some degree, as shown in Fig. 2

Table 2 Definitions of different working stages

Working condition	Systematic error / Magnitude	Random error / Magnitude
Case 1	Large / 30%*1	Large / 15%*1
Case 2	Medium / 20%	Medium / 10%
Case 3	Small / 10%	Small / 5%

*1: Percentage of error in sensor measurement

The errors in different ranges have no significant influence on the calibration results for whole calibration. All results are not ideal with a large error range from 1-1,000%. This is because there is only one distance function in whole calibration, and the function contains 7 offsetting constants and 3 unknown parameters. Simultaneously, each item (h_2, Q_c, Q_h) in the distance function construction contains normalizing and sensitivity normalizing coefficients. Under the condition of a certain amount of data, due to the above-mentioned various unknown quantities and uncertainty coefficients, the constraints between various parameters are significantly reduced, and all calibration results completely deviate from the true values during calibration.

Local calibration that applies the VIC method shows better results than whole calibration. By dividing the AHU system into two calibration domains, the first part only involves the mixed air phase. From the case 1-3 results, it can be observed that the mixed air temperature T_2, return air temperature T_6 and fresh air ratio Ra are calibrated. For these three systematic and random errors, the maximum error rate is 26.67%. However, it can be observed that the distance function contains only one term and there are too many unknown parameters. Hence, all parameters in the local domain 1 are not completely calibrated, resulting in a large deviation of 56% between mixed air humidity PHI_2 and return air humidity PHI_6. The variables calibrated in the local domain 1 need to be incorporated in local domain 2. However, due to the large error of the two parameters (PHI_2, PHI_6) in the local domain 1, the calibration results of the four variables (T_3, T_4, PHI_3, PHI_4) in local domain 2 all deviate significantly from the true values. In the local domain 2, the two terms in the distance function both contain M. Under multiple constraints, the deviation between the calibration result of M and the true value is less than 30%. In component calibration, the key idea of this study is that after all parameters are calibrated in the first component calibration domain, the obtained data close to the true values are incorporated into the next component calibration domain, and finally, all sensors are calibrated. Based on the steady-state model of the AHU system and several sets of steady-state measurements, all calibration results of component calibration are very close to the true values after applying Bayesian MCMC. This is because in the calibration process, the entire system is divided into five calibration domains, and the number of unknown parameters in each calibration domain is not more than three. In the calibration process, all sensors in the system are calibrated by incorporating the variables in the previous component into the next component after calibration, and the calibration is carried out in sequence with the deviation being less than 30%.

Through further depiction in Tables 3-5, it can be observed that the accuracy of the calibration results is significantly improved with the gradual reduction of the calibration domain range under the condition of a certain steady-state model and amount of data. Compared with whole calibration and local calibration, all the results of component calibration have a smaller fluctuation range and the deviation is below 30%. It can be observed that the size of the calibration domain division and the number of unknown parameters in the calibration domain significantly affects the accuracy of calibration. Hence, when the VIC method is applied for the calibration of complex building energy systems, component calibration can significantly improve the effectiveness of the diagnosis results and ensure the stable and reliable operation of building energy systems.

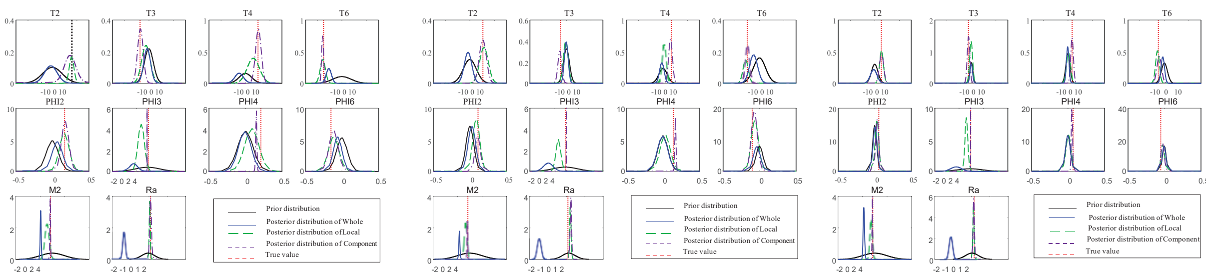

Fig.2. Calibration results of various sensors in Case 1-3

Table 3 Comparison of results before and after calibrations with various errors for Case 1

Sensor	Correction functions and variable	Virtual condition		Before calibration (prior distribution)		Whole calibration: After calibration (posterior distribution)			Local calibration: After calibration (posterior distribution)			Component calibration: After calibration (posterior distribution)		
		True value of sensor	True value of x	M*1	SD*1	M*1	SD*1	Deviation	M*1	SD*1	Deviation	M*1	SD*1	Deviation
T_2	$T_{c2}=T_2+x_{T2}$	26.5	7.95	0	3.975	-1.08	4.23	113.58%	7.85	0.96	1.26%	7.22	2.33	9.18%
T_3	$T_{c3}=T_3+x_{T3}$	12.2	-3.66	0	1.83	0.11	2.13	103.01%	-1.19	1.76	67.49%	-3.46	1.16	5.46%
T_4	$T_{c4}=T_4+x_{T4}$	17	5.1	0	2.55	-2.84	2.62	155.69%	3.21	2.52	37.06%	5.30	1.17	3.92%
T_6	$T_{c6}=T_6+x_{T6}$	25	-7.5	0	3.75	-8.55	1.74	14.00%	-7.80	1.06	4.00%	-8.19	2.69	9.20%
PHI_2	$PHI_{c2}=PHI_2+x_{PHI2}$	0.5494	0.1648	0	0.0824	0.078	0.086	52.67%	0.16	0.066	2.91%	0.17	0.051	3.16%
PHI_3	x_{PHI3}	-	0.95	0.9	1	-1.27	0.57	233.68%	0.38	0.27	60.00%	0.87	0.0026	8.42%
PHI_4	$PHI_{c4}=PHI_4+x_{PHI4}$	0.7	0.21	0	0.105	-0.0093	0.11	104.43%	0.087	0.098	58.57%	0.15	0.0077	28.57%
PHI_6	$PHI_{c6}=PHI_6+x_{PHI6}$	0.5	-0.15	0	0.075	-0.067	0.071	55.33%	-0.11	0.073	26.67%	-0.11	0.061	26.67%
M	x_M	-	0.8	1	1	0.092	0.049	88.50%	0.62	0.18	22.50%	0.80	0.027	0.00%
Ra	x_{Ra}	-	0.15	0.2	1	-1.01	0.22	773.33%	0.14	0.028	6.67%	0.14	0.047	6.67%

*1. M: Median value (systematic error), SD: Standard deviation (random error)

Table 4 Comparison of results before and after calibrations with various errors for Case 2

Sensor	Correction functions and variable	Virtual condition		Before calibration (prior distribution)		Whole calibration: After calibration (posterior distribution)			Local calibration: After calibration (posterior distribution)			Component calibration: After calibration (posterior distribution)		
		True value of sensor	True value of x	M*1	SD*1	M*1	SD*1	Deviation	M*1	SD*1	Deviation	M*1	SD*1	Deviation
T_2	$T_{c2}=T_2+x_{T2}$	26.5	5.3	0	2.65	-0.95	2.04	117.92%	5.79	1.76	9.25%	5.32	1.46	0.38%
T_3	$T_{c3}=T_3+x_{T3}$	12.2	-2.44	0	1.22	-0.012	1.03	99.51%	-0.30	1.01	87.70%	-2.71	0.79	11.07%
T_4	$T_{c4}=T_4+x_{T4}$	17	3.4	0	1.7	-0.59	1.26	117.35%	1.06	1.64	68.82%	3.06	0.78	10.00%
T_6	$T_{c6}=T_6+x_{T6}$	25	-5	0	2.5	-3.29	2.21	34.20%	-5.64	1.09	12.80%	-4.84	1.67	3.20%
PHI_2	$PHI_{c2}=PHI_2+x_{PHI2}$	0.5494	0.1099	0	0.0549	0.027	0.055	75.43%	0.088	0.048	19.93%	0.11	0.036	0.09%
PHI_3	x_{PHI3}	-	0.95	0.9	1	-1.13	0.54	218.95%	0.34	0.20	64.21%	0.99	0.0013	4.21%
PHI_4	$PHI_{c4}=PHI_4+x_{PHI4}$	0.7	0.14	0	0.07	-0.004	0.071	102.86%	0.029	0.069	79.29%	0.17	0.0078	21.43%
PHI_6	$PHI_{c6}=PHI_6+x_{PHI6}$	0.5	-0.1	0	0.05	-0.037	0.05	63.00%	-0.063	0.05	37.00%	-0.07	0.04	30.00%

M	x_M	-	0.8	1	1	0.12	0.043	85.00%	0.59	0.12	26.25%	0.81	0.033	1.25%
Ra	x_{Ra}	-	0.15	0.2	1	-1.31	0.34	973.33%	0.13	0.035	13.33%	0.14	0.038	6.67%

*1. M: Median value (systematic error), SD: Standard deviation (random error)

Table 5 Comparison of results before and after calibrations with various errors for Case 3

Sensor	Correction functions and variable	Virtual condition		Before calibration (prior distribution)		Whole calibration			Local calibration			Component calibration		
						After calibration (posterior distribution)			After calibration (posterior distribution)			After calibration (posterior distribution)		
		True value of sensor	True value of x	M*1	SD*1	M*1	SD*1	Deviation	M*1	SD*1	Deviation	M*1	SD*1	Deviation
T_2	$T_{c2}=T_2+x_{T2}$	26.5	2.65	0	1.325	-0.57	1.79	121.51%	2.79	0.77	5.28%	2.79	0.86	5.28%
T_3	$T_{c3}=T_3+x_{T3}$	12.2	-1.22	0	0.61	-0.058	0.66	95.25%	-0.10	0.60	91.80%	-1.15	0.54	5.74%
T_4	$T_{c4}=T_4+x_{T4}$	17	1.7	0	0.85	0.0039	0.68	99.77%	0.23	0.83	86.47%	1.70	0.55	0.00%
T_6	$T_{c6}=T_6+x_{T6}$	25	-2.5	0	1.25	-0.87	0.95	65.20%	-2.81	0.78	12.40%	-2.12	0.95	15.20%
PHI_2	$PHI_{c2}=PHI_2+x_{PHI2}$	0.5494	0.0549	0	0.0275	0.0054	0.028	90.16%	0.031	0.024	43.53%	0.036	0.021	34.43%
PHI_3	x_{PHI3}	-	0.95	0.9	1	-0.61	0.61	164.21%	0.59	0.12	37.89%	0.93	0.0013	2.11%
PHI_4	$PHI_{c4}=PHI_4+x_{PHI4}$	0.7	0.07	0	0.035	-0.0004	0.035	100.57%	0.0083	0.035	88.14%	0.054	0.0075	22.86%
PHI_6	$PHI_{c6}=PHI_6+x_{PHI6}$	0.5	-0.05	0	0.025	-0.0045	0.025	91.00%	-0.022	0.024	56.00%	-0.025	0.022	50.00%
M	x_M	-	0.8	1	1	0.11	0.057	86.25%	0.70	0.10	12.50%	0.81	0.027	1.25%
Ra	x_{Ra}	-	0.15	0.2	1	-1.22	0.29	913.33%	0.11	0.030	26.67%	0.13	0.034	13.33%

*1. M: Median value (systematic error), SD: Standard deviation (random error)

5. Conclusion

Based on the correlation between various sensors in the building energy system and the basic conservation laws, the virtual in-situ calibration is used to detect and correct the systematic and random error of sensors in the AHU system simultaneously. This method constructs the benchmark and correction function for all the sensors and inserts them into the distance function. By employing the Bayesian theory and MCMC methods, the offsetting constants and unknown parameters are estimated. The accuracy of calibration results is usually determined by the size of calibration domain and sensor error. In this study, whole calibration, three different local calibrations, and component calibration are incorporated into the air handling unit system with various combinations of systematic and random errors (large, medium, small). Some detailed conclusions could be drawn as follows:

1. For the systematic and random error of various sensors, the component calibration method is the most accurate, the whole calibration method is the least accurate, and three local calibrations lie in between. The maximum error of whole, local and component calibration reaches 973%, 112.7% and 30%, respectively.
2. The uncertainty of sensitivity and normalizing coefficients in the distance function has a great influence on the calibration results. For the whole and local calibration methods, the constraints between various parameters are significantly reduced because of the random and uncertain coefficients, and consequently most of correction results deviate from the true values.

References

[1] Revi, A., Climate change risk: an adaptation and mitigation agenda for Indian cities. Environment and urbanization, 2008. **20**(1): p. 207-229.

[2] Lau, S., et al., High-density, high-rise and multiple and intensive land use in Hong Kong: A future city form for the new millennium. Future forms and design for sustainable cities, 2005: p. 153-166.

[3] Amasyali, K. and N.M. El-Gohary, A review of data-driven building energy consumption prediction studies. Renewable and Sustainable Energy Reviews, 2018. **81**: p. 1192-1205.

[4] Kingma, B. and W. van Marken Lichtenbelt, Energy consumption in buildings and female thermal demand. Nature climate change, 2015. **5**(12): p. 1054.

[5] Huo, T., et al., China's energy consumption in the building sector: A Statistical Yearbook-Energy Balance Sheet based splitting method. Journal of cleaner production, 2018. **185**: p. 665-679.

[6] Käding, C., et al. Fine-tuning deep neural networks in continuous learning scenarios. in Asian Conference on Computer Vision. 2016. Springer.

[7] Kerdan, I.G., et al., ExRET-Opt: An automated exergy/exergoeconomic simulation framework for building energy retrofit analysis and design optimisation. Applied energy, 2017. **192**: p. 33-58.

[8] Yang, T., et al., An automated optimization method for calibrating building energy simulation models with measured data: Orientation and a case study. Applied energy, 2016. **179**: p. 1220-1231.

[9] Yu, Y., D. Woradechjumroen, and D. Yu, A review of fault detection and diagnosis methodologies on air-handling units. Energy and Buildings, 2014. **82**: p. 550-562.

[10] Gao, D.-c., et al., A system-level fault detection and diagnosis method for low delta-T syndrome in the complex HVAC systems. Applied energy, 2016. **164**: p. 1028-1038.

[11] Wang, Z., et al., Fault detection and diagnosis of chillers using Bayesian network merged distance rejection and multi- source non-sensor information. Applied energy, 2017. **188**: p. 200-214.

[12] Li, G., et al., A sensor fault detection and diagnosis strategy for screw chiller system using support vector data description-based D-statistic and DV-contribution plots. Energy and Buildings, 2016. **133**: p. 230-245.

[13] Du, Z., X. Jin, and Y. Yang, Fault diagnosis for temperature, flow rate and pressure sensors in VAVsystems using wavelet neural network. Applied energy, 2009. **86**(9): p. 1624-1631.

[14] Castrup, M., et al., Metrology: Calibration and measurement processes guidelines. 1994.

[15] Zhengwei, L. and H. Gongsheng, Preventive approach to determine sensor importance and maintenance requirements. Automation in Construction, 2013. **31**: p. 307-312.

[16] Kato, T., Perturbation theory for linear operators. Vol. 132. 2013: Springer Science & Business Media.

[17] Yoon, S. and Y. Yu, Extended virtual in-situ calibration method in building systems using Bayesian inference. Automation in Construction, 2017. **73**: p. 20-30.

[18] Yoon, S. and Y. Yu, Strategies for virtual in-situ sensor calibration in building energy systems. Energy and Buildings, 2018. **172**: p. 22-34.

[19] Yoon, S. and Y. Yu, Hidden factors and handling strategies on virtual in-situ sensor calibration in building energy systems: Prior information and cancellation effect. Applied energy, 2018. **212**: p. 1069-1082.

[20] Yu, Y. and H. Li, Virtual in-situ calibration method in building systems. Automation in Construction, 2015. **59**: p. 59-67.

[21] Yoon, S. and Y. Yu, Hidden factors and handling strategy for accuracy of virtual in-situ sensor calibration in building energy systems: Sensitivity effect and reviving calibration. Energy and Buildings, 2018. **170**: p. 217-228.

[22] Wang, P., et al., Automated reviving calibration strategy for virtual in-situ sensor calibration in building energy systems: Sensitivity coefficient optimization. Energy and Buildings, 2019.

[23] Kim, Y.-J., S.-H. Yoon, and C.-S. Park, Stochastic comparison between simplified energy calculation and dynamic simulation. Energy and Buildings, 2013. **64**: p. 332-342.

[24] Ramin, M. and G.B. Arhonditsis, Bayesian calibration of mathematical models: Optimization of model structure and examination of the role of process error covariance. Ecological informatics, 2013. **18**: p. 107-116.